scientific reports

Check for updates

OPEN

Application and mechanistic insights of a washing/microwave/ultrasonic ternary pretreatment for enhancing barite flotation in waste drilling fluids

Yu Xia[1,2,3,4]✉, Hui Mao[4], Shanfa Tang[1,2,3]✉, Shuixiang Xie[4]✉, Hongbo Liu[5], Wen Ren[4] & Mingdong Zhang[4]

A quantity of recoverable barite exists in high-density waste drilling fluid. Based on the inefficiencies and complexities of existing recycling methods, a novel pre-treatment approach which includes clean-breaking, high-speed washing, ultrasonic dispersion, and microwave heating and a new depressant (Gellan Gum) was proposed. The floatability, separation efficiency and mechanism were discussed by SEM, adsorption capacity, zeta potential measurements and contact angle tests. The results of reverse flotation experiments results indicated that secondary water washing proves highly effective in enriching a significant quantity of barite solid phase. Subsequent microwave-ultrasonic and flotation can obtain barite of high quality with recovery and density reaching 81.5% and 4.238 g/cm^3, respectively. It can be utilized directly in the preparation of drilling fluid. Mechanism studies shown that the per-treatments substantially enhances the barite grade while effectively eliminating low-density solid phases adhering to the barite surface, thus exposing additional contact points between the constituents so as to improve flotation separation. This new recovery scheme has environmental advantages and great reference value for the separation of barite within high-density waste drilling fluids.

Keywords Barite, High-density waste drilling fluid, Washing-microwave-ultrasonic, Flotation, Mechanism

As a pivotal global strategic mineral resource, barite finds extensive applications in petrochemical, medical protection, textiles, and construction materials owing to its specific gravity, non-toxic nature, non-magnetic properties, and ability to absorb various types of radiation[1,2]. In ultra-deep drilling, 85 ~ 90% of barite is frequently used as a weighting agent in drilling mud, particularly in the booming 10,000 m ultra-deep drilling sector. There is a substantial demand for barite in ultra-deep drilling wells, accompanied by a significant quantity of high-density waste drilling fluids returned to drainage[3,4]. According to statistics, only a single well, the annual production of high-density waste drilling fluid can be up to 1 million tons, which contains a large number of barite solid phase to provide sufficient aggravating agent resources, the recovery of barite in high density waste drilling fluids not only can alleviate the tension of barite resources, but also to respond to today's global decarbonization, and build green water and green mountains of the concept of environmental protection[5,6].

The structure of domestic high-density waste drilling fluid barite reuse equipment has evolved gradually from simplicity to integrated and intelligent systems. The first-generation barite reuse system primarily includes a cyclone. High-density waste drilling fluid enters the cyclone inlet under pressure and speed, where the material separates along the cyclone wall due to differences in density and particle size, moving axially downward and

[1]School of Petroleum Engineering, Yangtze University, Wuhan 430100, China. [2]Hubei Key Laboratory of Oil and Gas Drilling and Production Engineering, Yangtze University, Wuhan 430100, Hubei Province, China. [3]School of Petroleum Engineering, Yangtze University: National Engineering Research Center for Oil & Gas Drilling and Completion Technology, Wuhan 430100, China. [4]CNPC Research Institute of Safety and Environmental Technology Co. Ltd, Beijing 102206, China. [5]State Key Laboratory of Environmental Criteria and Risk Assessment, Chinese Research Academy of Environmental Sciences, Beijing 100012, China. ✉email: xydsb1997@163.com; tangsf2005@126.com; hbxsx168@126.com

radially outward, achieving separation of mixtures with different densities. However, this system's simplicity limits its ability to process complex components of drilling fluid barite effectively[7]. The second generation introduced a multi-stage reuse system that integrates two centrifuges in series through an organic linkage system, dividing the process into multiple stages to handle drilling fluids. The rotational speed of the centrifuge is controlled to enhance barite recovery[8,9]. Currently in China, the predominant process combines cyclone separation, vibration desanding, multiple centrifuges, and solid–liquid separation. This process, although effective with a recovery rate of ≥ 80% and a processing capacity of about 2 m^3/h, typically results in recovered barite containing approximately 15% low-density solid phase inclusions[10–12]. Recovering barite with particle sizes less than 74 μm and fine low-density solid phase particles is challenging with low processing capacity. Often, density adjustment of recovered barite and blending with commercially available barite are necessary, leading to economic losses and procedural complexities, failing to fully meet operational requirements. Foreign high-density waste drilling fluid treatment equipment is characterized by a more complex structure and higher integration level compared to domestic equipment. Typically employing a combination of chemical and physical treatment methods, it includes dosing tanks for adding surfactants and flocculants to pretreat mud, facilitating easier subsequent mud treatment processes[13]. The primary distinction between foreign and domestic recycling processes lies in the foreign method's utilization of chemical pretreatment and barite flotation within the combined process, significantly enhancing barite grade and density. The effectiveness of this technology in recovering barite hinges on the pretreatment process's quality and the selectivity of flotation chemicals, with varying recovery outcomes for different drilling fluid components. Thus, maintaining stable pretreatment processes and ensuring robust selectivity of flotation chemicals are critical aspects of this technology[14,15].

Wang[16] et al. innovatively employed gellan gum (GG) as a selective inhibitor and incorporated sodium oleate (NaOl) to achieve concentrates. This groundbreaking approach resulted in an impressive recovery rate of 85.24% and a remarkable CaF_2 grade of 86.73% at a pH of 7.5. Guo J[17] et al. conducted a barite pure mineral flotation test, probing into the impact of sodium oleate on barite floatability under microwave radiation. The results revealed that microwave heating enhances the positive electric properties of the barite surface, consequently augmenting its specific surface area. This phenomenon, in turn, elevates the adsorption rate of sodium oleate on the barite surface, ultimately amplifying the efficiency of flotation recovery. Lev O[18] et al. used ultrasonic treatment followed by flotation for the selective separation of KCl and NaCl in saturated salt solution. Under the experimental conditions of ultrasonic treatment power of 10–75 W and resonance frequency of 20 kHz, the recovery of NaCl from potassium concentrate was reduced from 17.9 to 9.9%, and the recovery of KCl was increased from 89.9 to 95.9%, which realized the selective separation of different substances.

From the above study, it can be seen that a variety of processes such as microwave radiation and ultrasound can effectively promote flotation and enhance the recovery effect, while the addition of selective inhibitor chemicals is also the key to flotation experiments. Hence, this paper advances a central theme incorporating a diverse array of processes and novel chemicals. It proposes the utilization of a "high speed washing + microwave radiation + ultrasonic dispersion" ternary synergistic pretreatment combination process. Additionally, the study draws insights from the report on innovative chemicals, such as GG, serving as a flotation inhibitor. The approach embraces the counter-flotation method for the recovery of barite from high-density waste drilling fluids. The entire process is characterized by its cleanliness, conciseness, and operational simplicity. The chemicals employed align with environmentally friendly principles and are easily accessible. This comprehensive investigation of the recovery mechanism seeks to contribute a viable thought process for the recuperation of barite mineral resources.

Materials and methods

Materials

High-density waste drilling fluid, discharged centrifugally from shale gas wells in southwestern China (with original densities ranging from 2.0–2.2 g/cm^3); the specimens were treated by drying, crushing, grinding, and sieving, from which 3–5 g of product within the −0.075 mm range was chosen as the representative specimen. The XRD pattens of high-density waste drilling fluid is shown in (Fig. 1a). The content of barite in the high-density waste drilling fluid is as high as 52.41%, and the low-density impurity solid phase is mainly calcite, dolomite and quartz.

In order to determine the elemental composition and morphological characteristics of the sample surface more accurately, the high-density waste drilling fluid was analyzed by SEM-EDS through field emission scanning electron microscope S-4800.The morphology and elemental composition of the samples are depicted in (Fig. 1) and (Table.1), respectively.

It can be seen that distinct spatial disparities among the internal barite and assorted low-density solid phases within the sample, manifesting a disarrayed distribution (Fig. 1b); the waste drilling fluid' surface exhibits pronounced roughness attributable to the adhesion of varying proportions of dissimilarly shaped low-density solid phases to barite (Fig. 1c). Moreover, the low-density solid phases predominantly exist within a mosaic of finely grained or micro-fine-grained inclusions (Fig. 1d), posing considerable challenges for complete dissociation and recovery. Spectroscopic analysis indicates the presence of Ba (white), Si (green), Ca (red), Al (yellow), Fe (blue), and Mg (purple) within the sample, and they are evenly distributed in the specimens. Elemental ratios are presented in Table. 1, revealing that the predominant elements in the samples are Ba, Ca, and Mg, while Al, Fe, and Mg are present in lower proportions. Based on the elemental composition and combined with the XRD analysis results, it can be confirmed that the composition of the low-density solid phases in the high-density waste drilling fluids is, in descending order, including quartz (SiO_2), calcite ($CaCO_3$), and taraspite ($CaMg(CO_3)_2$).

Clean gel breaker YJ-I, provided by School of Petroleum Engineering, Yangtze University; Gellan gum, industrial grade, Shandong Fengtai Bio-technology Co.

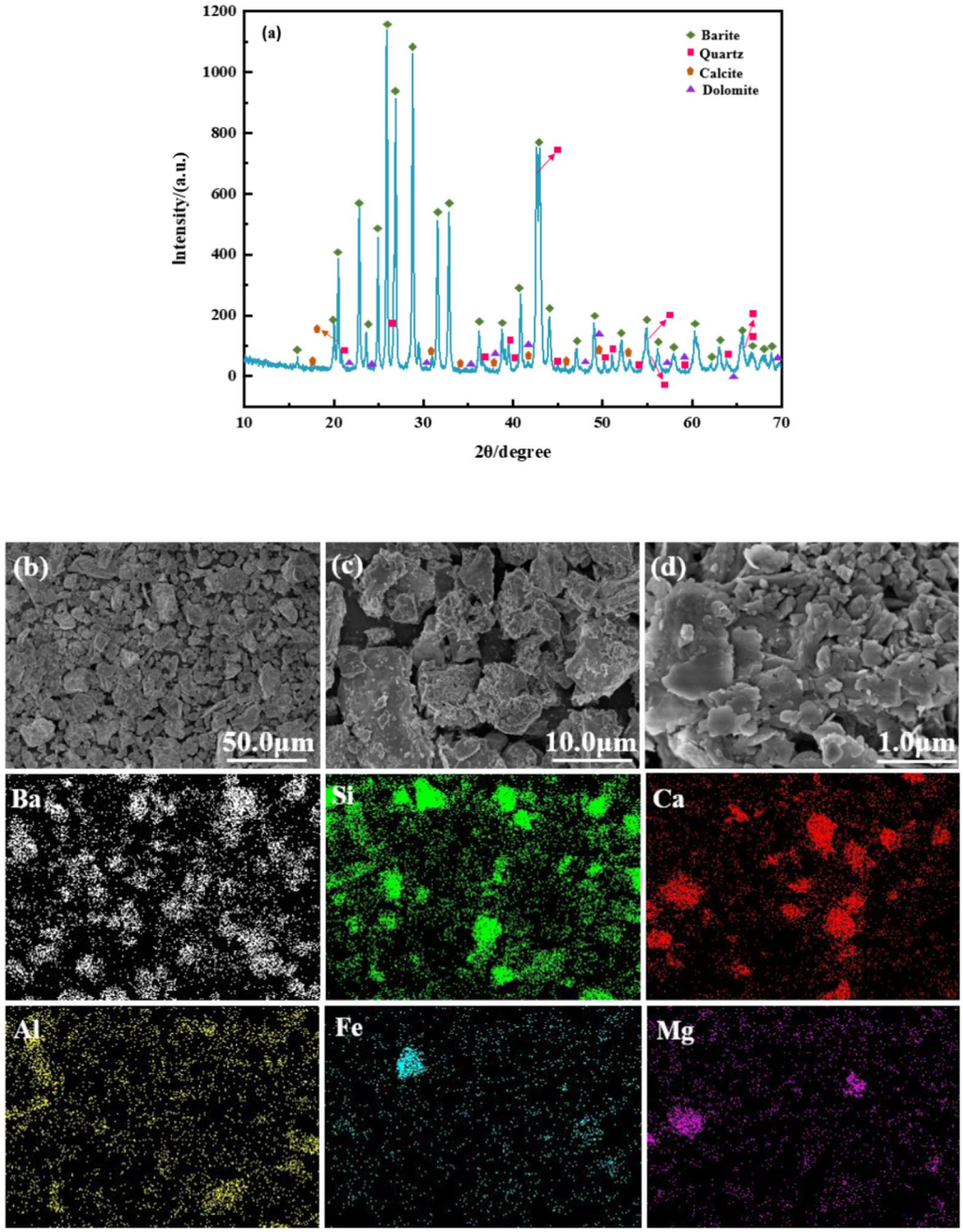

Fig. 1. (**a**) XRD pattens of high-density waste drilling fluid; (**b**–**d**) SEM images of High-density waste drilling fluid and elemental maps of the High-density waste drilling fluid that show the distributions of Ba, Si, Ca, Al, Fe and Mg.

Elements	Ba	Si	Ca	Al	Fe	Mg
Weight percentage/%	52.41	24.20	10.03	5.60	4.46	3.30

Table 1. The element proportion of the high-density waste drilling fluid.

Equipment

1.0 L single-tank flotation machine XFD-III, Wuhan Prospecting Machinery Co., Ltd; Spiral cleaner JB-I, provided by School of Petroleum Engineering, Yangtze University; Microwave oven G80W23CSP-Z (output power, 800 W; rated microwave power, 2450 MHz); Ultrasonic cleaning machine KQ3200E, frequency 40 kHz, rated power 150 W; Electronic balance, Shanghai Ltd; Nanoparticle and zeta potential analyzer (LitesizerTM500),

Occhio Instruments (Beijing) Co., Ltd; Optical wetting angle meter (OSA200), Ningbo New Boundary Scientific Instruments Co. Ltd; UV Spectrophotometer, Shanghai Yitian Precision Instrument Co., Ltd; Field Emission Scanning Electron Microscope S-4800, Hitachi (China) Co., Ltd; Laboratory Compact Pulverizer BF-10, Hebei Benchen Technology Co; Portable pH meter PHB-4, Beijing Airan Technology Co., Ltd; D/max 2500 X-ray diffractometer, Rigaku Co., Ltd; Rock crusher SE-750, Yongkang Shengxiang Electric Appliances Co., Ltd; DHG-9203A Electric thermostatic drying oven, Shanghai Jinghong Experimental Equipment Co; Lee's Specific Gravity Bottle, Anhui Weiss Experimental Equipment Co.

Methods

Barite pre-enrichment experiment

The primary enrichment:1 L of high-density waste drilling fluid is introduced into the spiral cleaner JB-I, followed by the addition of 1, 2 or 3 L of water to maintain the solid/liquid ratio at 1:1, 1:2 or 1:3, respectively. The mixture was added 5‰ of clean gel breaker, YJ-I, and stirred for 20 min at 1000 r/min. After settling for 5 min, the solid phase beneath the 1 cm cover layer was separated, while the sediment at the bottom of the vessel was gathered as the targeted sample for barite recovery. The quantitative sample was transferred into a beaker and subjected to drying in an electric thermostatic drying oven at 105 °C for a duration of 12 h. Upon completion of the drying procedure, the sample was cooled at room temperature, and its density was assessed utilizing a Lee's specific gravity bottle.

The secondary enrichment: the precipitate obtained from the primary enrichment is separated and introduced into 1, 2 or 3 L of water, followed by the repetition of the procedure.

Ultrasonic-microwave treatment experiment

A 200 g sample of the enriched barite mixture was subjected to microwave heating treatment in a G80W23CSP-Z microwave oven. After the treatment, it was retrieved and allowed to cool to room temperature. Following this, deionized water was added to create a barite mixture with a solid–liquid ratio of 1:4. The mixture was then subjected to ultrasonic pre-treatment in a KQ3200E ultrasonic cleaner for 5–20 min in preparation for the subsequent flotation test.

Waste drilling fluid flotation experiment

After microwave-ultrasonic treatment, the barite mixture was transferred to the flotation tank. The pH value of slurry was adjusted using a 10% HCl solution. After a 10-min settling period, the inhibitor and trapping agent (with the option to include a small amount of auxiliary foaming agent if needed) were introduced sequentially. The mixture underwent a 6 min inflation and flotation procedure. The whole experimental procedure of the flotation experiment is displayed in (Fig. 2). The mixed concentrate product obtained in the flotation tank underwent drying and weighing to calculate the recovery rate of barite.

Mechanism exploration experiment

SEM test. The solid phase mixture of barite, both before and after undergoing secondary washing-microwave-ultrasonic treatment, was subjected to drying, grinding, and sieving through a 200-mesh sieve. Subsequently,

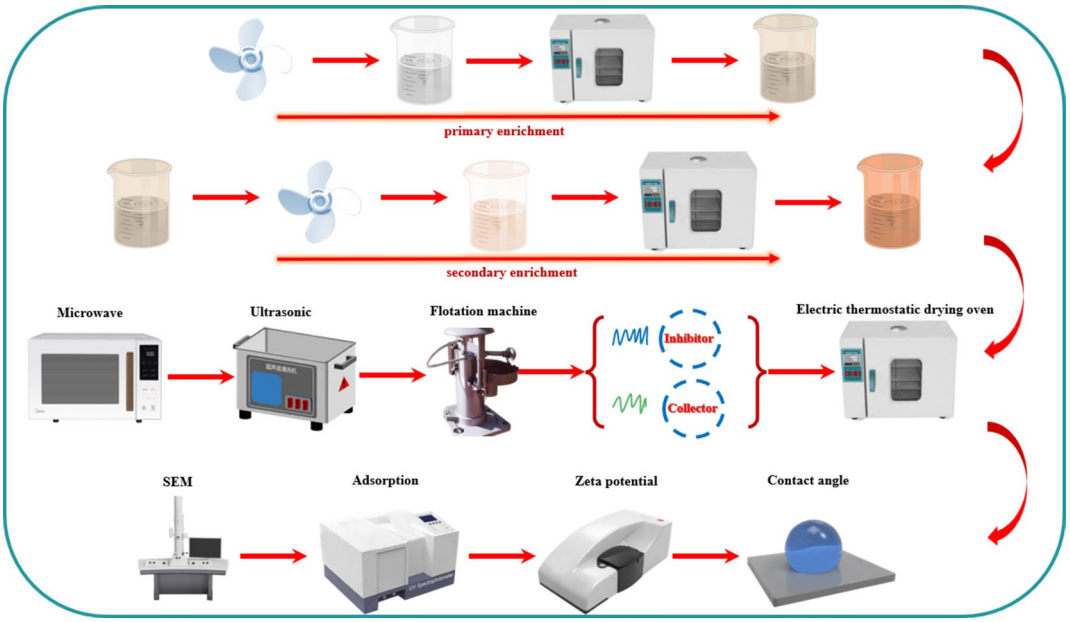

Fig. 2. Barite recovery experiments procedure of high-density waste drilling fluids.

3–5 g of specimens were selected for micro-morphology testing utilizing a field emission scanning electron microscope S-4800.

Adsorption amount determination. Upon completion of the flotation procedure, 3–5 ml of the upper layer of the clear liquid were aspirated, followed by utilizing a UV-visible spectrophotometer to measure the corresponding absorbance. Subsequently, the adsorption amount of sodium dodecyl sulfate was calculated using formula (1):

$$\tau = \frac{C_0 - C_e V}{m} \tag{1}$$

where τ—sodium dodecyl sulfate adsorption amount, mg/g; C_0—Sodium dodecyl sulfate concentration, mg/L; C_e—supernatant sodium dodecyl sulfate concentration, mg/L; V—volume of solution, L; m—mass of barite mixture, g.

Zeta potential measurement. A 2.0 g sample of recovered barite is precisely weighed and subsequently ground to achieve a particle size of less than 5 μm. Deionized water and flotation chemicals are added to the sample as necessary for the flotation process, followed by stirring and allowing the mixture to stand for 10 min. Once the settling process was concluded, the supernatant was extracted and subsequently injected into the cuvette of the potentiometric analyzer for potentiometric analysis. Three measurements were conducted for each sample, and the resultant average value was computed. The calculated average is deemed as the ultimate outcome.

Contact angle measurement. The surface of the sample was dispersed and subsequently dried using ultrasonic vibration. Following this, the sample was submerged in deionized water at pH 7.5 and subjected to sequential treatment with the desired flotation reagent solution, with each treatment lasting for 3 min. The surfaces of the samples were meticulously rinsed with deionized water and subsequently dried during each immersion. Once the drying process was finished, the samples were subjected to testing using optical wetting angle meter (OSA200). During the determination of the contact angle, a drop of deionized water was dispensed onto the surface of the sample via an auto-injector, and the contact angle was measured after the drop had reached stability. Three tests were conducted for each sample, and the resulting average value was considered as the ultimate outcome.

Results and discussion

Barite pre-enrichment experiments before and after breaking gum-washing

High-density waste drilling fluid is a sol-gel suspension mixed system composed of oil and water as the dispersing medium, clay, viscosity builder, filter loss reduction agent, a variety of inorganic salts and aggravating agent as the dispersing phase, and must be subject to a certain amount of gel-breaking treatment before flotation[19]. Therefore, in this study, a clean and strong oxidizing gum breaker YJ-I was added to firstly break the gums of high-density waste drilling fluids and subsequently enrich the barite by high-speed washing. The effect of the secondary enrichment of breaking gum-washing on the mixed solid-phase density of recovered barite is shown in (Table 2). The results show that, under the experimental conditions of a rotational speed of 1000r/min, a gum breaker amount of 5‰, and a solid–liquid ratio of 1:2, primary enrichment enhances the mixed solid-phase density of barite by approximately 11% points. Furthermore, the mixed solid-phase density of barite before and after secondary enrichment increases by about 13.8% points, highlighting the significant purification effect of secondary enrichment.

To further validate the efficacy of secondary enrichment on barite purification, the morphological attributes of the recovered solid-phase barite were examined both before and after secondary enrichment, utilizing the aforementioned conditions. Figure 3 illustrates the morphological changes observed in the solid-phase barite samples. Initially, the dry sample of the original waste drilling fluid exhibited a black hue with coarse particles, predominantly forming agglomerates (Fig. 3a)[20]. Following primary water washing, there was a noticeable enhancement in both the color and particle size of the mixed solid phase of barite, rendering it light black in color (Fig. 3b). Subsequent secondary water washing further refined the particle size, resulting in the mixed solid phase of barite exhibiting a light black hue with a hint of pale white coloration, albeit with evident small agglomerates on the surface (Fig. 3c). The alteration in color and particle size of the mixed solid phase of barite can be attributed to the high-speed water washing process, which interacts with the low-speed water. The enhancement in both color and particle size observed in the recovered barite mixed solid phase could potentially stem from the substantial density disparity between barite and the low-density solid phase during the high-speed water washing process. Barite was mainly distributed in large quantities in the outer layer near the wall, whereas the

Enrichment times	Barite mixed solid phase density/(g·cm^{-3})
None	3.628
Once	4.036
Twice	4.127

Table 2. The effect of breaking gum-washing on barite recovery from high-density waste drilling fluids.

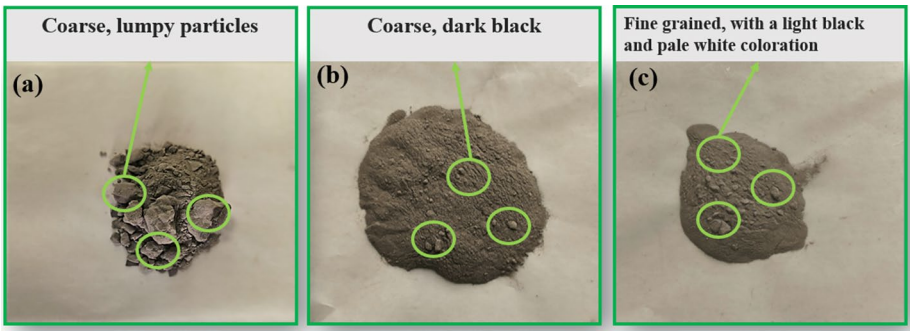

Fig. 3. Comparison of recovered barite before and after broken rubber washing; (**a**) Dry sample of raw waste drilling fluid; (**b**) barite after primary enrichment; (**c**) barite after secondary enrichment.

low-density solid phase is primarily concentrated in the inner layer. Upon cessation of spiral cleaner rotation, the low-density solid phase, owing to differing settling velocities, becomes entrapped between the uppermost water layer and the lowermost barite layer, thereby facilitating effective separation. As the proportion of low-density solid phase diminishes within the barite layer, the color gradually transitions to white. With successive washings, the progressive reduction in low-density solid phase content culminates in continuous improvement in barite purity, resulting in increasingly white chromaticity and finer particle sizes[21].

The results suggest that secondary enrichment is indeed more efficient in purifying barite. However, as an independent physical method, it faces challenges in achieving optimal barite separation efficiently. With an increase in the number of enrichment cycles, despite resulting in a slight improvement in barite purity, there ensued notable wastage of resources and human labor, alongside a substantial deterioration in the actual quality of the recovered barite. Thereby augmenting the method's uncertainty[22]. Consequently, further investigation into subsequent chemical processes is imperative.

Barite flotation experiment in drilling waste fluid before and after microwave-ultrasonic pretreatment

Effect of concentration of SDS and pH value on barite flotation recovery and barite quality

Under the conditions of ultrasonic-microwave pretreatment and the addition of 0.07% SDS, the flotation performance was investigated across various collector concentrations and pH values. The results are shown in (Fig. 4a,b).

Figure 4a illustrates the impact of SDS concentration on the flotation performance of barite. Observation of Fig. 4a reveals a gradual increase in both barite recovery and mixed solid phase density with rising SDS concentration. The peak values for both barite flotation recovery and mixed solid phase density occurred at an SDS concentration of 0.05%, reaching 80.4% and 4.232 g/cm^3, respectively. A slight decline in barite recovery was observed as SDS concentration continued to increase, which may be due to the non-selective trapping of SDS, and too much SDS will improve the wettability of barite and low-density solid phase at the same time, making them both more hydrophobic, so that part of barite was flown to the surface with the low-density solid phase, which resulted in the decrease of barite recovery and density[23].

Figure 4b illustrates the impact of pH variations on the flotation performance of barite. As evident from Fig. 4b, both barite recovery and the density of the barite mixed solid phase escalated with rising pH levels. At a pH value of 8.0, both barite flotation recovery and the density of the barite mixed solid phase peaked at 80.4% and 4.232 g/cm^3, respectively. With further increases in pH, there was a slight decline observed in both barite recovery and the density of the barite mixed solid phase. This phenomenon may be attributed to the increased presence of OH^- ions in the slurry at higher pH levels, leading to enhanced adsorption of OH^- ions on the surface of the low-density solid phase. Consequently, this enhances the hydrophilicity of the surface of the low-density solid phase, thereby hindering the adsorption of trapping anions[24].

Effect of time and microwave power on barite flotation recovery and barite quality

Microwaves are a form of electromagnetic radiation characterized by frequencies ranging from 300 MHz to 300 GHz[25,26]. Due to their properties of penetration, selective heating, low thermal inertia and absorption, microwaves find widespread applications in substance heating, microwave extraction, microwave grinding and microwave floatability. Yu investigated the impact of microwaves on the interaction between deionized water, slurry and the trapping mechanism in fluorite flotation. The study showed that microwaves can enhance mineral flotation recovery through the trapping mechanism. Consequently, the microwave pretreatment process was incorporated to explore the potential enhancement of barite recovery and density. The results are shown in (Fig. 4c-d).

The results showed that after the microwave pretreatment, the flotation indexes of barite were all increased to a certain extent, and the recovery rate of barite was higher than 78% under the microwave time of 20–60 s and the microwave power of 200–800 W, and the density of recovered barite was higher than 4.200 g/cm^3, which indicated that the microwave treatment could have a certain promotional effect on the flotation[27]. In the range of microwave time from 20 to 60 s, the flotation indexes increased rapidly when the microwave time was increased

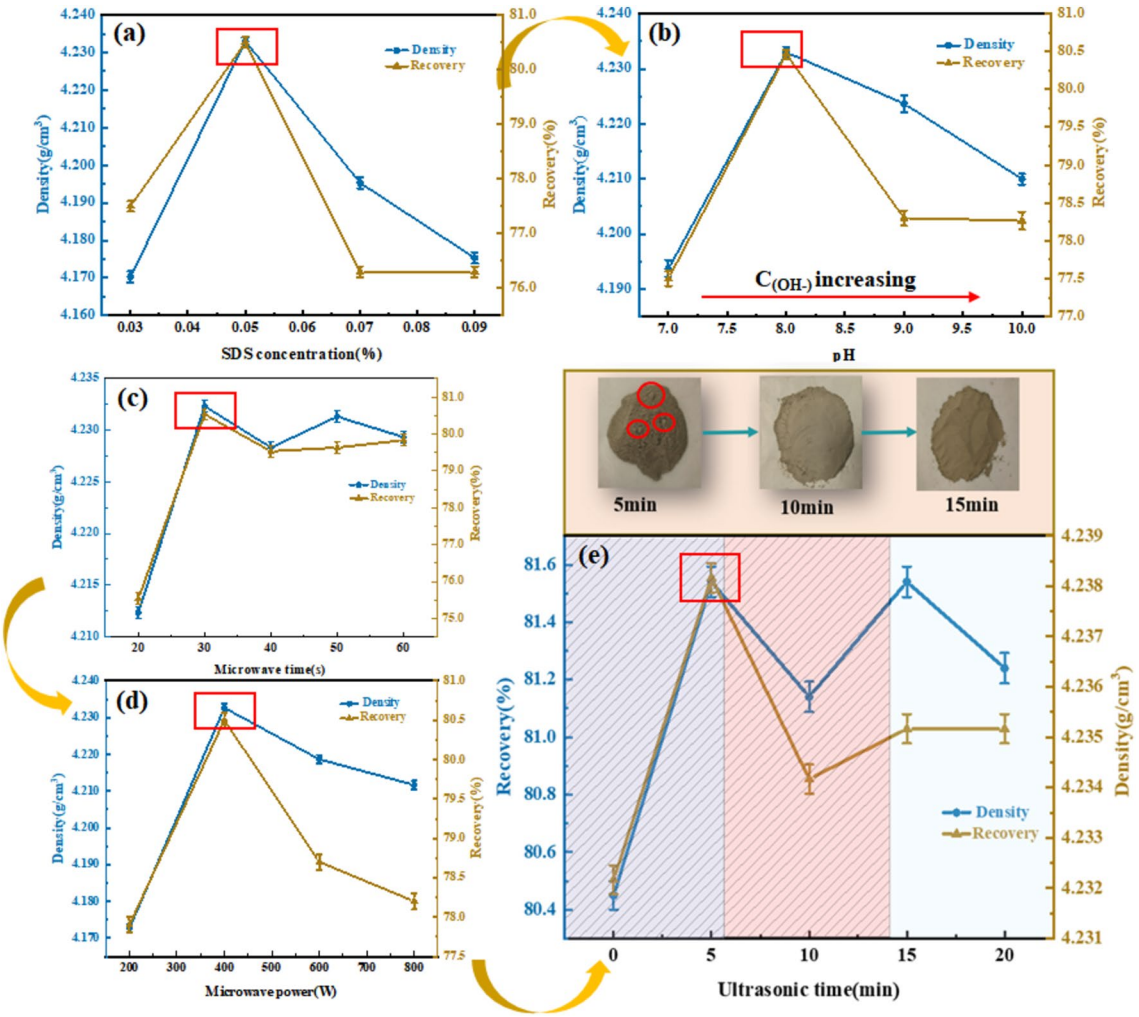

Fig. 4. (**a**) Effect of various SDS concentrations on the flotation recovery of barite; (**b**) Effect of various pH values on the flotation recovery of barite; (**c**) Effect of various microwave time on the flotation recovery of barite; (**d**) Effect of various microwave power on the flotation recovery of barite; (**e**) Effect of various ultrasonic time on the flotation recovery of barite.

from 20 to 30 s. However, when the microwave time continued to be increased after 30 s, the barite recovery indexes showed a small fluctuation, and thereafter no further change. With the increase of microwave power, the barite recovery index increased rapidly at 200–400 W, but showed a small decrease as the microwave power continued to increase. This trend can be attributed to the coexistence of barite and low-density solid phase in high-density waste drilling fluid. Increasing the microwave time and intensity can increase the specific surface area of barite to activate flotation and partially desorb these two phases to improve flotation. However, it cannot be completely dissociated, and too long microwave time and too high microwave intensity will lead to partially dissociated tiny barite and low-density solid-phase mixtures can be easily brought to the liquid surface by bubbles for simultaneous flotation due to their small mass and volume, resulting in low flotation efficiency. Therefore, reasonable adjustment of microwave treatment time and intensity to control the particle size of the treated mixed solid phase is the key to promote flotation. The peak recovery of barite (recovery = 80.4%, density = 4.232 g/cm^3) was achieved at a microwave time of 30 s and a microwave power of 400 W, respectively.

Effect of microwave-ultrasonic synergistic pretreatment on barite flotation recovery and barite quality

Ultrasound is a technique that employs acoustic energy to uniformly disperse particles in a liquid. Typically utilizing ultrasonic frequencies (greater than 20 kHz), it can be conducted using either an ultrasonic bath or an ultrasonic probe. Ultrasonic waves induce the formation of vacuum bubbles (voids) within the liquid, which subsequently expand and implode with considerable force, a phenomenon known as cavitation. This process yields various effects including emulsification, dispersion, particle size reduction, and homogenization[28]. This section delves into investigating the impact of ultrasonic treatment duration on barite flotation, conducted under the optimal conditions delineated in Sect. "Effect of time and microwave power on barite flotation recovery and barite quality", with the results presented in (Fig. 4e).

The results indicate a substantial increase in both barite recovery and the density of the mixed solid phase of barite with prolonged ultrasonic treatment time, suggesting the promotional impact of ultrasonic pretreatment on flotation. Upon increasing the ultrasonic treatment time from 0 to 5 min, the optimal flotation performance was attained (recovery = 81.5%, density = 4.238 g/cm^3), with minimal influence observed on the flotation performance with further increases in ultrasound duration.

A detailed study of the images depicting barite recovery after 0, 5, and 10 min of ultrasonication reveals that the barite sample obtained post-ultrasonication exhibits a powdery consistency, with scant evidence of prominent lumps or solid chunks on the surface layer. This observation suggests that ultrasonication facilitates a more thorough separation of the mixed solid phase of barite. Furthermore, upon comparing the barite recovered after 5 and 10 min of ultrasound treatment, minimal disparity in the quality of the recovered barite between the two durations is observed.

The above trend can be attributed to the increase in the adsorption capacity of barite by ultrasonic pretreatment, which increases the adsorption rate of barite to flotation chemicals. Furthermore, given that the mixed solid phase of barite post-microwave treatment assumes an irregular lumpy form characterized by heightened micropores and cracks, the cavitation bubbles generated during ultrasound can infiltrate these irregular lumps, inducing their fragmentation and disintegration[29]. This phenomenon facilitates more effective removal of the low-density solid phase in barite and enhances the efficacy of flotation chemicals. The separation process gradually reaches completion with increasing ultrasonic treatment duration. As pretreatment entails a dual process resulting in the refinement of the barite mixture, reducing the duration of ultrasonic treatment achieves both removal effects. Subsequent prolongation of ultrasonic treatment time yields marginal improvements in separation efficiency. As depicted in (Fig. 5e), the optimal recovery (recovery = 81.5%, density = 4.238 g/cm^3) was attained with an ultrasonic treatment duration of 5 min.

Analysis of flotation mechanism before and after ultrasonic-microwave pretreatment

Comparison of SEM images of barite surface before and after different pretreatments

The SEM images of the barite surface after various pretreatments are shown in (Fig. 5a–f). Following washing, a higher presence of irregular particles adheres to the barite surface (Fig. 5a). The overall morphology exhibits a relatively rough and lumpy distribution (Fig. 5d), with noticeable rises and pits. Nevertheless, the overall purity is increased, suggesting that water washing enables a comparatively pure separation between barite and the low-density solid phase, albeit with limited separation effectiveness[30]. During the removal process, the barite and the low-density solid phase collide with each other at high speeds, resulting in deep and shallow pits and cracks in the recovered barite mixed solid phase. Hence, a single high-speed water washing pretreatment alone remains insufficient to achieve complete separation, necessitating the implementation of additional auxiliary processes.

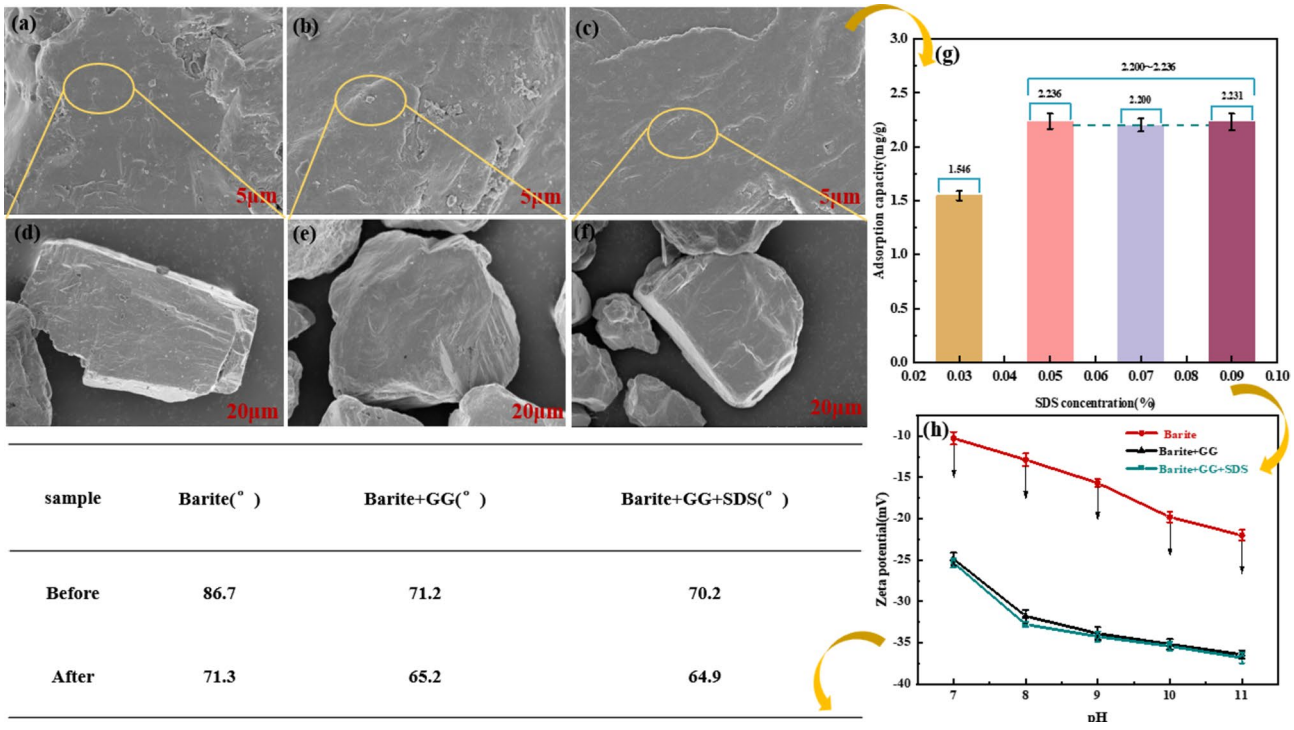

sample	Barite(°)	Barite+GG(°)	Barite+GG+SDS(°)
Before	86.7	71.2	70.2
After	71.3	65.2	64.9

Fig. 5. (**a**–**f**) SEM images of recovered barite mixed concentrate under different treatment conditions; secondary enrichment (a-5 and d-20 μm), secondary enrichment + microwave (b-5 and e-20 μm), secondary enrichment + microwave + ultrasonic (c-5 and f-20 μm); (**g**) Adsorption capacities of SDS under different concentrations on the barite surfaces; (**h**) Zeta potentials of barite as a function of various pH and changes in contact angle of barite before and after the action of GG and SDS.

After microwave treatment, irregular cracks appeared on the surface of barite (Fig. 5b), and some projections were partially dislodged to form small spheres (Fig. 5e) with a slight decrease in diameter. This phenomenon is due to the barite mixed solid phase in the microwave electromagnetic field, due to its own magnetic loss and dielectric loss, the absorption of electromagnetic energy into internal energy, inducing the internal thermal effect of its own particles, so that the particles are rapidly subjected to thermal expansion, and the release of its thermal stresses promotes the growth and expansion of the cracks on the surface of the barite mixed solid phase as well as the interfacial friction and fragmentation between its different structures, which promotes the desorption of the low-density solid phase[31].

The density and smoothness of the barite surface increased after ultrasonic treatment (Fig. 5c), while the diameter decreased. This is because the ultrasonic pretreatment on the one hand can destroy the adsorption of low-density solid phase on the surface of barite, on the other hand, can cause fatigue damage to the low-density solid phase and be stripped, the vibration of the gas-type bubbles on the surface of the barite scrubbing, once the low-density solid-phase attached to the surface of the seam can be drilled, the bubbles immediately drilling vibration to make the low-density solid-phase detachment[32]. Ultrasound propagation in the cleaning fluid will produce positive and negative alternating acoustic pressure, forming a jets, impacting the cleaning parts, while due to the nonlinear effect will produce acoustic and micro-acoustic flow, and ultrasonic cavitation at the interface of solids and liquids will produce high-speed micro-jets, all of these roles, able to destroy the low-density solid phase, removing or weakening the boundary layer, increasing the agitation, diffusion, resulting in the microwave treatment process of the adhering residual solid phase shedding, which improves the purity (Fig. 5f)[33].

Determination of the adsorption of trapping agent on barite surface

Investigating the adsorption capacity of SDS on the barite surface can provide insights into the mechanisms underlying traps and inhibitors affecting both barite and the low-density solid phase. The results are shown in (Fig. 5g).

The observed amount of SDS adsorbed on the barite surface amounted to 1.546 mg/g upon addition of SDS without the inhibitor GG. Furthermore, saturation of adsorption on the barite surface was attained as the SDS concentration escalated from 0.03 to 0.05%, with subsequent increments in SDS concentration yielding minimal alterations in adsorption levels[34,35]. Owing to the fragile Ba–O bonds within the barite structure, facile breakage occurs, facilitating the chemical adsorption of Ba^{2+} ions and dodecyl sulfate on the barite surface. This process leads to the formation of relatively stable barium dodecyl sulphate compounds on the barite surface with alkyl orientated towards the surrounding medium. Consequently, the hydrophobicity of the barite surface is enhanced, promoting its flotation upwards[36]. Analogously, metal ions present on the surface of the low-density solid phase can form stable compounds with dodecyl sulfate, resulting in the inefficient separation of barite from the low-density solid phase. Thus, the introduction of a selective inhibitor is imperative to shield the barite. The environmentally friendly selective inhibitor GG harbors a plethora of reactive functional groups, including carboxyl and hydroxyl groups[37]. Given that these reactive functional groups readily interact with multivalent metal sites on the mineral surface. Upon addition of GG, the ionized Ba^{2+} ions on the barite surface exhibit a pronounced affinity for binding with the active functional groups (–COO and –OH), resulting in robust chemisorption of GG onto barite. This phenomenon effectively impedes the subsequent adsorption of SDS on the barite surface, leading to a notable decrease in the floatability of barite and facilitating the floatability-based separation of barite from the low-density solid phase. Thus, this further corroborates the selective inhibition of barite by GG, underscoring its indispensable role in this flotation experiment.

Zeta potential analysis before and after microwave-ultrasound pretreatment

Zeta potential changes in minerals during the flotation process are often associated with reagent adsorption[38]. Therefore, zeta potential measurements were performed to elucidate the adsorption behaviors of reagents on barite surfaces. Figure 5h illustrates the alterations in surface charge experienced by barite following interaction with various reagents. As depicted, the zeta potential of barite exhibits a negative charge. Following treatment with GG, the zeta potential of barite consistently shifted towards negativity across the pH range examined, suggesting adsorption of GG onto the barite surface[39]. At pH = 8.0, the zeta potential of barite exhibited a negative shift of 20.0 mV, indicative of robust adsorption of GG onto the barite surface. Conversely, at pH = 7.0 or pH > 8.0, the change in zeta potential of barite ranged from 12.3 to 18.7 mV, suggesting that the adsorption of GG onto barite is most pronounced at pH = 8. The zeta potential of barite exhibited minimal change following the subsequent addition of SDS, with a shift of < 3.5 mV from pH 7.0 to 11.0, indicative of the pronounced hindrance imposed by prior GG adsorption on the subsequent SDS adsorption onto the barite surface[40]. Consequently, the zeta potential findings suggest that GG significantly obstructs the adsorption of SDS onto the barite surface.

Surface wettability of barite under different agent treatments before and after microwave reaction

The surface wettability of minerals plays a crucial role in their interaction with air bubbles, thereby directly influencing flotation performance[41,42]. Typically, surface wettability is assessed through the measurement of mineral contact angles, with higher contact angles generally indicative of greater floatability. In this study, the surface wettability of barite was assessed under varying agent conditions both before and after microwave treatment, with the results delineated in (Fig. 5).

The results revealed that the contact angles of barite prior to and following microwave treatment were 86.7 and 71.3°, respectively. Following GG treatment, there was a notable decrease in the contact angle of barite, decreasing from 86.7° and 71.3 to 71.2° and 65.2° before and after microwave treatment, respectively. This observation suggests effective adsorption of GG molecules onto the barite surface, resulting in a discernible reduction in barite floatability[43]. Subsequently, SDS was introduced, and the contact angle of barite remained nearly unchanged

before and after microwave treatment. This result suggests that the presence of GG significantly influences the subsequent attachment of SDS onto the barite surface, likely attributed to the enhanced chemical adhesion of GG onto the barite surface, potentially in the form of Ba-OH or Ba-COOH[44]. This phenomenon could explain the reduced floatability of barite with a high recovery rate. Consequently, GG demonstrated enhanced adhesion to barite, leading to a substantial hindrance in the adsorption of SDS onto the barite surface.

Analysis of the mechanism of promoting barite flotation under water-washing microwave and ultrasonic pretreatment conditions

In order to have a clearer understanding of the mechanism of reagents' action on the mineral surface in pretreatment and flotation, the whole purification mechanism of barite was demonstrated as in (Fig. 6). The clean gum breaker YJ-I through oxidation can firstly destroy the colloidal structure in the drilling fluid, reduce the viscosity of the drilling fluid, and enhance the fluidity of the drilling fluid in the subsequent high-speed water washing[45]. Due to the water dilution and centrifugal force, centrifugal process of barite solid phase most of the slurry settled in the lower part of the wall near the machine position, when the machine stops rotating, the slurry inside the machine at this time is divided into three layers, from top to bottom, respectively, for the water layer, low-density solid phase mixing layer, barite mixing layer, and remove the uppermost layer of the water layer, excluding the surface layer of the low-density solid phase mixing layer, at this time a more pure barite mixed solid phase can be obtained[46]. According to the above purification process and adjusting the number of washing times, purer barite mixed solid phase can be obtained.

Based on the close combination of barite and the lumpy solid formed by the low-density solid phase, it is difficult to carry out effective separation by direct flotation. Therefore, microwave pretreatment was introduced, and the mixed solid phase of barite under microwave radiation showed graded thermal response characteristics, in the main stage of thermal response of barite, a large amount of moisture evaporates from barite, generating gas pressure, causing pore expansion and crack extension; in the main stage of thermal response of externally adhered low-density solid phase, the low-density solid phase absorbs the microwave energy, resulting in the removal of low-density solid phase, and the cracks are extended and through the pores, and the moisture and the migration of the low-density solid phase leads to a large number of pore and fissure generation, and provides a channel for the removal of moisture and the desorption of the low-density solid phase. As a result, desorption between barite and low-density solid phase is formed[47].

Subsequently, under the influence of ultrasonic waves, the minuscule bubbles lodged within the pores and fissures of both barite and the low-density solid phase in the slurry swiftly collapse.

The local instantaneous temperature increase and pressure change are induced, which help to break the adsorption chemical bond between barite and low-density solid phase particles, thus promoting the dissociation between the two and exposing more sites[48]. Simultaneously, ultrasonic waves create feeble vortices and eddies in the slurry, generating miniature water currents. These currents expedite the movement of surfactant molecules towards the solid–liquid interface, which enabling faster adsorption and subsequent separation from the surface of the low-density solid phase.

Following a comprehensive pretreatment involving water washing, microwave irradiation, and ultrasonic treatment, the residual low-density solid phase adhering to the barite surface was entirely dislodged, thereby establishing an optimal flotation environment[49]. Due to the selective inhibition exerted by GG. It interacts with Ba^{2+} ions on the barite surface through hydrophilic functional groups (–COOH, –OH), forming a protective

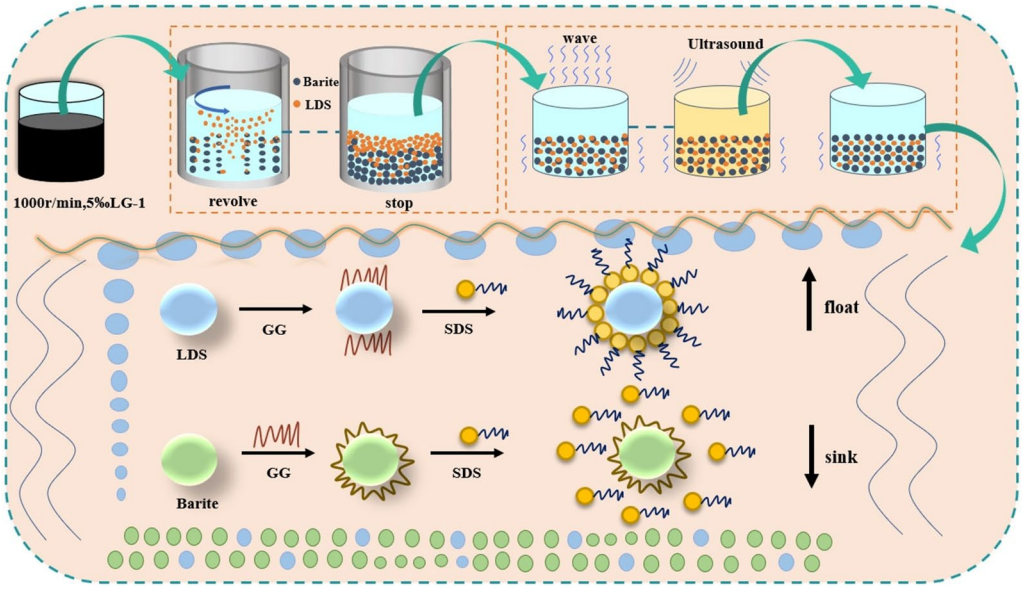

Fig. 6. Mechanism of barite recovery based on the whole process of washing-microwave-ultrasonic pretreatment and flotation.

capping layer which hinders the direct interaction between SDS and the barite surface, effectively shielding the active sites on the barite surface. Consequently, the collector fails to efficiently adsorb onto the barite, thereby enhancing the flotation efficiency.

Conclusions

(1) Employing a rotational speed of 1000 r/min, a concentration of 5‰ clean breaker LG-1, and a solid–liquid ratio of 1:2, the secondary enrichment effect before and after breaking-washing was elevated by approximately 13.8%. Consequently, a mixed solid phase containing barite with a density of 4.127 g/cm^3 was achievable;
(2) In experimental settings with GG and SDS additions of 0.07 and 0.05%, microwave pretreatment for 30 s at 400W, pH value maintained at 8.0, and ultrasonication for 5 min, the barite recovery rate and mixed solid-phase density achieved peak values of 81.5% and 4.238 g/cm^3;
(3) Mechanism analysis: The secondary washing-microwave-ultrasonic pretreatment facilitated the desorption of barite and the low-density solid phase, markedly improving the attachment state of the mixed mineral surface with barite. This exposure of additional contact sites facilitated the chemical adsorption of GG and SDS onto the surfaces of barite and the low-density solid phase, respectively. Moreover, it reduced the wettability of the barite surface. Additionally, GG comprehensively encapsulated the barite, resulting in a robust inhibition, thereby facilitating flotation separation.
(4) This study focuses on high-density waste drilling fluid from shale gas wells as the experimental subject. Future applications of this technology require broader verification to establish its universality. Developing microwave and ultrasonic equipment for pilot scale-up in the field is essential to validate its practical efficacy. Moreover, given the varied compositions of group waste drilling fluids, the selective inhibitory effectiveness of GG varies, necessitating ongoing exploration of novel green and efficient inhibitors for achieving stable recycling outcomes.

Data availability

The datasets used and/or analyzed during the current study available from the corresponding author on reasonable request.

Received: 1 June 2024; Accepted: 28 August 2024
Published online: 07 September 2024

References

1. Yang, T., Wang, N., Gu, H. & Guo, T. Froth flotation separation of carbon from barium slag: Recycling of carbon and minimize the slag. *Waste Manag.* **120**, 108–113. https://doi.org/10.1016/j.wasman.2020.11.022 (2021).
2. Liu, C. *et al.* Utilization of water glass as a dispersant to improve the separation performance of fluorite from barite slimes. *Coll. Surf. A* **635**, 128036. https://doi.org/10.1016/j.colsurfa.2021.128036 (2022).
3. Mikos-Szymańska, M. *et al.* Characterization of drilling waste from shale gas exploration in central and Eastern Poland. *Environ. Sci. Pollut. Res.* **25**(36), 35990–36001. https://doi.org/10.1007/s11356-018-2365-8 (2018).
4. Peng, Y., Li, W., Hu, J. & Li, J. Study and application of a method for evaluating the performance of barite recycling. *Drill Fluid Complet. Fluid* **35**(4), 57–61. https://doi.org/10.3969/j.issn.1001-5620.2018.04.010 (2018).
5. Liu, C. *et al.* The utilization of citric acid as a depressant for the flotation separation of barite from fluorite. *Miner. Eng.* **156**, 1064. https://doi.org/10.1016/j.mineng.2020.106491 (2020).
6. Nguyen, T. *et al.* Pre-concentration of fluorite from a rare earth element carbonatite deposit through the combination of magnetic separation and leaching. *Miner. Eng.* **174**, 106998. https://doi.org/10.1016/j.mineng.2021.106998 (2021).
7. Wang, C., Lu, Y., Qi, H., Luo, X. & He, L. Flotation mechanism and performance of air/condensate bubbles for removing oil droplets in the presence of acetic acid. *Sci. Total Environ.* **927**, 172311. https://doi.org/10.1016/j.scitotenv.2024.172311 (2024).
8. Sun, H., Niu, F. & Zhang, J. Investigation on the flotation separation of smithsonite from calcite using calcium lignosulphonate as depressant. *Coll. Surf. A* **630**, 127571. https://doi.org/10.1016/j.colsurfa.2021.127571 (2021).
9. Dong, L., Jiao, F., Qin, W. & Liu, W. Selective flotation of scheelite from calcite using xanthan gum as depressant. *Miner. Eng.* **138**, 14–23. https://doi.org/10.1016/j.mineng.2019.04.030 (2019).
10. Yang, S. *et al.* The anionic flotation of fluorite from barite using gelatinized starch as the depressant. *Coll. Surf. A* **597**, 124794. https://doi.org/10.1016/j.colsurfa.2020.124794 (2020).
11. Molaei, N., Razavi, H. & Chelgani, S. Designing different beneficiation techniques by taguchi method for upgrading Mehdi-Abad white barite ore. *Min. Proc. Ext. Met. Rev.* **39**(3), 198201. https://doi.org/10.1080/08827508.2017.1399889 (2017).
12. Mohamed, A., Basfar, S., Elkatatny, S. & Ai-majed, A. Pre-vention of barite sag in oil- based drilling fluids using a mix-ture of barite and ilmenite as weighting material. *Sustainability* **11**(20), 5617–5630. https://doi.org/10.3390/su11205617 (2019).
13. Smaha, R., He, W., Sheckelton, J., Wen, J. & Lee, Y. Synthe-sis-dependent properties of barlowite and Zn-su bstituted barlowite. *J. Solid State Chem.* **268**, 123–129. https://doi.org/10.1016/j.jssc.2018.08.016 (2018).
14. Wu, Q., Chi, K., Wu, Y. & Lee, S. Mechanical, flamma-ble, and thermal performances of co- extruded wood polymer composites with core: shell structure containing barite-filled shells. *Wood Sci. Technol.* **54**(5), 1299–1318. https://doi.org/10.1016/j.matdes.2014.04.010 (2014).
15. Zhou, Z. *et al.* The genesis of the dahebian Zn-Pb deposit and associated barite mineralization; implications for hydrothermal fluid venting events along the Nanhua Basin South China. *Ore Geol. Rev.* **101**, 785–802. https://doi.org/10.1016/j.oregeorev.2018.08.013 (2018).
16. Wang, L., Lyu, W., Huang, L., Li, F. & Zhang, H. Utilization of gellan gum as a novel eco-friendly depressant in the flotation separation of fluorite from barite. *Miner. Eng.* **184**, 107640. https://doi.org/10.1016/j.mineng.2022.107640 (2022).
17. Guo, J., Wen, M. & Wu, J. Mechanistic study on the flotation of barite with $C_{18}H_{33}NaO_2$ under microwave radiation based on UV-visible spectrophotometric analysis. *Physicochem. Probl. Miner. Process.* **58**(6), 156349. https://doi.org/10.37190/ppmp/156349 (2022).
18. Lev, O., Inna, V., Odile, B., Tatyana, P. & Oskar, O. F. Intensification of the flotation separation of potash ore using ultrasound treatment. *Miner. Eng.* **171**, 107092. https://doi.org/10.1016/j.mineng.2021.107092 (2021).

19. Lv, W. *et al.* Enhancing classification and recovery of barite from waste drilling fluid by inlet particle arranging of hydrocyclone. *J. Water Process. Eng.* **156**, 104341. https://doi.org/10.1016/j.jwpe.2023.104341 (2023).
20. Bicalho, I., Santos, D., Ataíde, C. & Duarte, C. Fluid-dynamic behavior of flow in partially obstructed concentric and eccentric annuli with orbital motion. *J. Pet. Sci. Eng.* **137**, 202–213. https://doi.org/10.1016/j.petrol.2015.11.029 (2016).
21. Liu, H., Li, P., Xiao, H. & Mu, W. The fluid–solid coupling analysis of screw conveyor in drilling fluid centrifuge based on ANSYS. *Petroleum* **1**(3), 251–256. https://doi.org/10.1016/j.petlm.2015.07.009 (2015).
22. Marion, C. *et al.* The potential for dense medium separation of mineral fines using a laboratory falcon concentrator. *Miner. Eng.* **105**, 7–9. https://doi.org/10.1016/j.mineng.2016.12.008 (2017).
23. Sun, K. *et al.* Application and mechanism of anionic collector sodium dodecyl sulfate (SDS) in phosphate beneficiation. *Minerals* **7**(2), 29. https://doi.org/10.3390/min7020029 (2017).
24. Ni, C. *et al.* A novel collector with wide pH adaptability and high selectivity towards flotation separation of scheelite from calcite. *Miner. Eng.* **158**, 106606. https://doi.org/10.1016/j.mineng.2020.106606 (2020).
25. Ozkan, S., Baktarhan, Y., Gungoren, C. & Demir, I. Effect of conventional and microwave thermal treatments on floatability of low- and high-rank lignites. *Energ. Sour. Part A* **42**, 2357–2369. https://doi.org/10.1080/15567036.2019.1643426 (2019).
26. Wu, J., Li, J., Lin, J., Yi, S. & Su, W. Analysis of the influence mechanism of microwvave on barite flotation by infrared ftting spectroscop. *Spectrosc. Spect. Anal.* **41**(10), 3083–3091. https://doi.org/10.3964/j.issn.1000-0593(2021)10-3083-09 (2021).
27. Lu, G., Zhou, J., Li, Y., Zhang, X. & Gao, W. The influence of minerals on the mechanism of microwave-induced fracturing of rocks. *J. Appl. Geophys.* **180**, 104123. https://doi.org/10.1016/j.jappgeo.2020.104123 (2020).
28. Prajiapati, A. Sono-assisted electrocoagulation treatment of rice grain based distillery biodigester effluent: Performance and cost analysis. *Process Saf. Environ.* **150**, 314–322. https://doi.org/10.1016/j.psep.2021.04.030 (2021).
29. Videla, A. *et al.* Ultrasound treatment on tailings to enhance copper flotation recovery. *Miner. Eng.* **99**, 89–95. https://doi.org/10.1016/j.mineng.2016.09.019 (2016).
30. Han, G. *et al.* Deep separation of critical metals of Mo and Re from waste solution by stepwise precipitation flotation: Selective chelation underlying separation mechanism. *Sep. Purif. Technol.* **313**, 123492. https://doi.org/10.1016/j.seppur.2023.123492 (2023).
31. Dai, C., Chen, P., Yang, Y. & Sun, W. Selective flotation of ilmenite from titanaugite using 2-amino-1,3-propanediol as a novel depressant. *Coll. Surf. A* **681**, 132752. https://doi.org/10.1016/j.colsurfa.2023.132752 (2024).
32. Liu, C., Wang, Q. & Yang, S. Effects of barite size on the fluorite flotation using the reagent scheme of GS/NaOl. *Coll. Surf. A* **626**, 127101. https://doi.org/10.1016/j.colsurfa.2021.127101 (2021).
33. Kasomo, R. M. *et al.* Selective flotation of rutile from almandine using sodium carboxymethyl cellulose (Na-CMC) as a depressant. *Miner. Eng.* **157**, 106544. https://doi.org/10.1016/j.mineng.2020.106544 (2020).
34. Han, W., Zhu, Y., Liu, J. & Li, Y. A novel depressant HPAM of the hematite in reverse cationic flotation of iron ore. *Coll. Surf. A* **641**, 128547. https://doi.org/10.1016/j.colsurfa.2022.128547 (2022).
35. Chen, X., Gu, G., Liu, D. & Zhu, R. The flotation separation of barite-calcite using sodium silicate as depressant in the presence of sodium dodecyl sulfate. *Physicochem. Probl. Miner. Process* **55**(2), 346–355. https://doi.org/10.5277/ppmp18136 (2017).
36. Gong, X. *et al.* Flotation separation of dolomite and brucite via selective adsorption of the inhibitor tetrasodium hydroxyethylphosphate. *J. Cent. S. Univ.* **30**, 2574–2586. https://doi.org/10.1007/s11771-023-5417-2 (2023).
37. Osmalek, T., Froelich, A. & Tasarek, S. Application of gellan gum in pharmacy and medicine. *Int. J. Pharm.* **466**(1), 328–340. https://doi.org/10.1016/j.ijpharm.2014.03.038 (2014).
38. Liu, C., Zhu, G., Song, S. & Li, H. Flotation separation of smithsonite from quartz using calcium lignosulphonate as a depressant and sodium oleate as a collector. *Miner. Eng.* **131**, 385–391. https://doi.org/10.1016/j.mineng.2018.11.045 (2019).
39. Li, L. *et al.* Flotation performance and adsorption mechanism of malachite with tert-butylsalicylaldoxime. *Sep. Purif. Technol.* **210**, 843–849. https://doi.org/10.1016/j.seppur.2018.08.073 (2019).
40. Yin, Z. *et al.* Depressing behaviors and mechanism of disodium bis (carboxymethyl) trithiocarbonate on separation of chalcopyrite and molybdenite. *Trans. Nonferr. Meta Soc.* **27**(4), 883–890. https://doi.org/10.1016/S1003-6326(17)60100-6 (2017).
41. Wang, Y. *et al.* Synthesis and utilization of a novel oleate hydroxamic acid collector for the flotation separation of bastnaesite from barite. *Miner. Eng.* **204**, 108405. https://doi.org/10.1016/j.mineng.2023.108405 (2023).
42. Chipfunhu, D., Zanin, M. & Grano, S. Flotation behaviour of fine particles with respect to contact angle. *Chem. Eng. Res. Des.* **90**(1), 26–32. https://doi.org/10.1016/j.cherd.2011.06.021 (2012).
43. Cui, Y., Jiao, F., Wei, Q., Wang, X. & Dong, L. Flotation separation of fluorite from calcite using sulfonated lignite as depressant. *Sep. Purif. Technol.* **242**, 116698. https://doi.org/10.1016/j.seppur.2020.116698 (2002).
44. Yang, B. *et al.* Improving flotation separation of apatite from dolomite using PAMS as a novel eco-friendly depressant. *Coll. Surf. A* **597**, 124794. https://doi.org/10.1016/j.mineng.2020.106492 (2020).
45. Sun, L., Geng, X., Song, T. & Zhang, Y. Response surface optimization of biosafety disposal of waste water based drilling fluids for deep drilling. *Drill Fluid Complet. Fluid* **39**(3), 327–333. https://doi.org/10.12358/j.issn.1001-5620.2022.03.010 (2022).
46. Xu, Y., Xu, D. & Zhang, X. Application of drilling fluid zero-discharge technology in bailu lake multi-well pad. *Drill Fluid Complet. Fluid* **33**(6), 63–67. https://doi.org/10.3696/j.issn.1001-5620.2016.06.011 (2016).
47. Parapari, P., Irannajad, M. & Mehdilo, A. Effect of acid surface dissolution pretreatment on the selective flotation of ilmenite from olivine and pyroxene. *Int. J. Miner. Process* **167**, 49–60. https://doi.org/10.1016/j.minpro.2017.07.017 (2017).
48. Wang, K. *et al.* Flotation separation of polyethylene terephthalate from waste packaging plastics through ethylene glycol pretreatment assisted by sonication. *Waste Manag.* **105**, 309–316. https://doi.org/10.1016/j.wasman.2020.02.021 (2020).
49. Huang, J. *et al.* Efficient selective flotation separation of fluorite from calcite using ferrous and ferric species as combined depressant. *Miner. Eng.* **205**, 108451. https://doi.org/10.1016/j.mineng.2023.108451 (2024).

Acknowledgements

Financial support from PetroChina,s Strategic and Forward-looking Major Science and Technology Project (2021DJ6601) is gratefully acknowledged.

Author contributions

Y. X：Writing—Original Draft，Validation，Investigation，Conceptualization H.M：Project administration, Supervision, Writing—Review & Editing, Conceptualization SF. T：Project administration，Supervision，R esources，Methodology SX X：Project administration，Funding acquisition，Methodology Resources HB. L：Investigation，Resources W.R：Investigation MD. Z：Investigation All authors reviewed the manuscript.

Competing interests

The authors declare no competing interests.

Additional information

Correspondence and requests for materials should be addressed to Y.X., S.T. or S.X.